

# PETROGENESIS OF QUATERNARY BASALTS IN SOUTHERN HANGAY MOUNTAINS, CENTRAL MONGOLIA: MANTLE SOURCE AND MAGMATIC EVOLUTION

---

ANGELA EKSTRAND

Beloit College

Sponsor: Jim Rougvie

TAMIR ENKHBAATAR

Mongolian University of Science and Technology

## INTRODUCTION

Alkaline volcanism of equivocal origin has occurred in a north-south belt throughout central Mongolia during the Cenozoic (Barry et al., 2003). This volcanism can be divided into two episodes, “watershed” or “plateau” flood basalts, occurring from 57 Ma to ~10 Ma, and “valley” basalts, occurring from ~6.5 Ma to the present (Devyatkin and Smelov, 1980). Several theories have been proposed regarding the origin of this volcanism, though none has been widely accepted (Barry et al., 2003). These theories include a mantle plume, and lithospheric delamination or a shallow thermal anomaly heating metasomatized lithosphere (Barry et al., 2003).

This study uses geochemical data to investigate the depth of the mantle source and the fractionation history of the younger “valley” basalts from the southern Hangay Nuruu (mountains) in central Mongolia. A comparison of this data with Barry et al. (2003) and Tielke et al. (this volume) allows for a broader picture of Mongolian volcanism and provides evidence to aid in the explanation of the origin of similar alkaline volcanics of central Asia, including Siberia, Russia, and China.

## METHODS

Lavas were sampled at seven sites, including five sites with flows and two sites with cinder cones (Fig. 1). Sections were measured at three

of the sites. One of the sites with volcanic centers (Site E) was mapped at a 1:20,000 scale.

Twenty-one samples were analyzed petrographically. These samples were analyzed for major and trace elements at Washington State University; all were analyzed by XRF, and 15 were also analyzed by ICP-MS.

## RESULTS

### FIELD DESCRIPTION/STRATIGRAPHY

Sections were measured at sites A, F, and H, individual flows not part of measured sections were sampled at sites B and C, and cones were sampled at sites D and E (Fig. 1). Based on descriptions of stratigraphy by Devyatkin and Smelov (1980), and their assertion that the youngest flows occur at the lowest elevations in valleys, the A section in the south is likely older than the northern flows. Northern sections F and H begin near to the valley floor, consistent with younger (Pliocene to Holocene) flows. Like sections F and H, section A is confined to its valley by the patterns of modern topography. However, section A spans a greater portion of the valley wall and begins further off the valley floor than the northern sections, suggesting it may be slightly older (Devyatkin and Smelov, 1980).

Section A (Fig. 1) is 130.5 m thick, begins ~30 m above the valley floor, has extensive cover between flows, and is characterized by dramatic changes in phenocryst phases, from olivine to

glomeroporphyritic plagioclase and pyroxene. Sections F (18.1 m thick) and H (70.4 m) are of limited extent, and are less voluminous than the A section (Fig 1.) They are composed of compound flows and display few changes in mineralogy. The dominant phenocryst in F is olivine, and in H is plagioclase.

Three samples were obtained from individual flows at site B (Fig. 1). The sample from site C (Fig. 1) is similar to the F and H flows in terms of mineralogy, and its flow is located on the valley floor.

Three cinder cones at site E are arranged in a line, with a dike striking  $304^\circ$ , at a bend in the Egiin Davaa fault, suggesting structural control of their location (Fig. 1). This clear structural association with the Egiin Davaa fault is also consistent with a younger (Pliocene to Holocene) age (Devyatkin and Smelov, 1980).

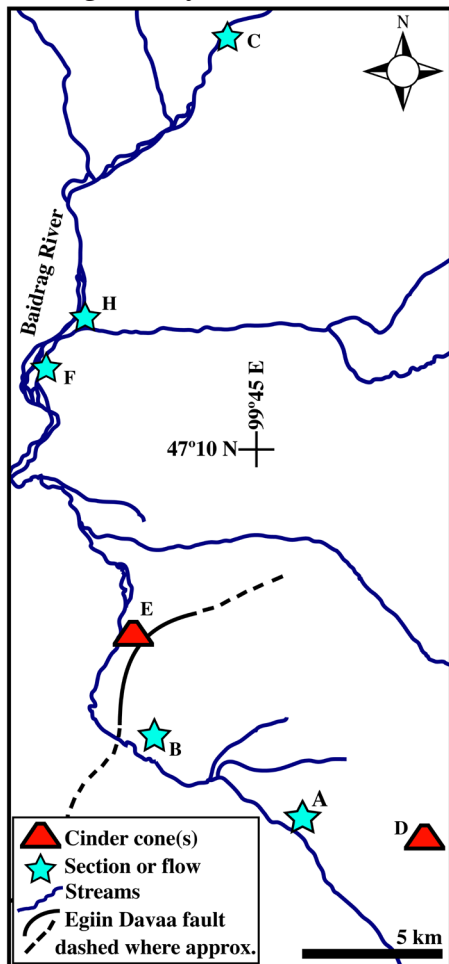


Figure 1. Map of study area. Down thrown block of the Egiin Davaa fault is to the northwest.

## PETROGRAPHY

Samples are porphyritic with an aphanitic groundmass. Olivine is the main phenocryst phase. Plagioclase does not occur as a phenocryst phase in most samples. Clinopyroxene and plagioclase are present as phenocrysts in H and toward the top of A. The groundmass mineral assemblage is predominantly plagioclase (50-70%), with olivine (10-20%), clinopyroxene (10-15%), and Fe-Ti oxides (5-15%).

Glomeroporphyritic texture is common, often including clinopyroxene. Samples from A are felty, while many from F and H are strongly trachytic. Clinopyroxene always displays oscillatory zoning, olivine is zoned with more Fe-rich rims and Mg-rich cores, and plagioclase commonly displays both continuous and oscillatory zoning. In every sample, olivine displays embayments indicative of resorption. Iddingsite commonly occurs in olivine. However, many samples show little iddingsitization, and other minerals in samples with altered olivine do not show alteration.

Xenocrysts are present in seven samples. Commonly, these consist of quartz inclusions with reaction rims containing radially oriented clinopyroxene and interstitial plagioclase. Inclusions in at least three other samples appear to be Al-rich pyroxenites with minor plagioclase and olivine. They are heavily reacted with the melt.

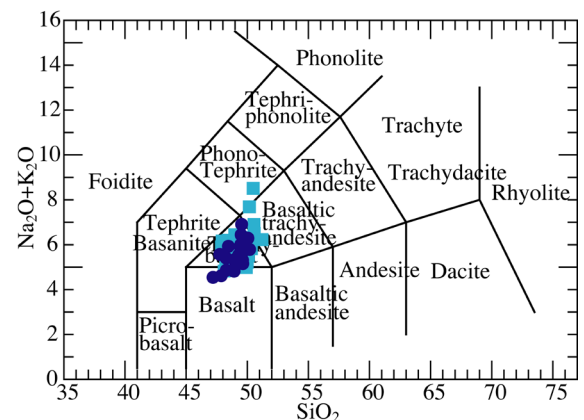
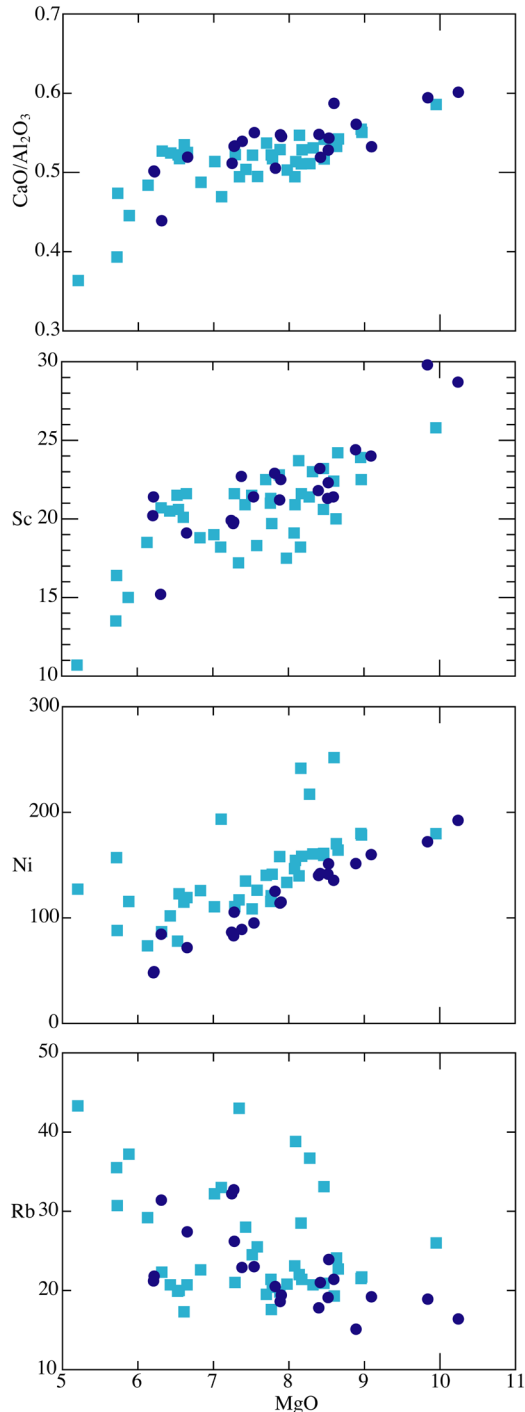


Figure 2. Total alkalis vs. silica diagram (after Le Bas et al., 1986). Dark blue circles, this study; light blue squares, Tielke et al. (this volume).

## GEOCHEMISTRY

All samples are alkaline. On the total alkali vs. silica diagram, four are basalts and 17 are trachybasalts, nine of which can be further classified as hawaiites (Fig. 2).  $\text{SiO}_2$  values range from 47.19-50.19 wt. %. Mg-numbers ( $100 \cdot \text{Mg}/(\text{Mg} + \text{Fe}^{2+})$ ) range from 52-66. All samples are nepheline-normative.



**Figure 3.** (Left) Fenner diagrams of MgO compared to  $\text{CaO}/\text{Al}_2\text{O}_3$ , Sc, Ni, and Rb. Dark blue circles, this study; light blue squares, Tielke et al. (this volume).

The samples show a positive correlation between MgO and CaO,  $\text{CaO}/\text{Al}_2\text{O}_3$ , Sc, Cr, and Ni.  $\text{K}_2\text{O}$ ,  $\text{Na}_2\text{O}$ ,  $\text{Al}_2\text{O}_3$ , Ba, and Rb negatively correlate with MgO (Fig. 3). Primitive mantle-normalized trace element patterns (Fig. 4) are more similar to average OIB than MORB. Patterns display high LILE, and LREE enrichment relative to HREE (Figs. 4, 5). Positive anomalies occur at Ba, K, and Sr. Pb has a wide distribution of values in the H section; other lavas have positive anomalies. All samples exhibit a small positive Eu anomaly.

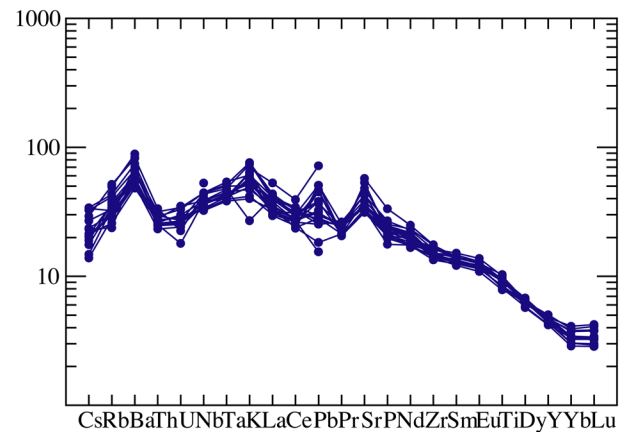


**Figure 4.** Whole-rock trace element concentrations normalized to primitive mantle (after Sun and McDonough, 1989).

Ce/Pb ratios range from 11 to 44. Ce/Pb <5 is consistent with crustal values, Ce/Pb ~9 is consistent with primitive mantle, and Ce/Pb ~25 is consistent with average mantle (Barry et al., 2003). La/Nb values range from 0.75 to 1.03. Higher values of ~1.5 and ~4.5 are consistent with upper and lower crust, respectively (Barry et al., 2003).

## DISCUSSION

### GEOGRAPHIC RELATIONSHIPS

Northern samples (localities C, F, and H; Fig. 1) show similar trace element patterns, with greater positive anomalies of Ba, K, and Sr. Southern samples (localities B, D, and E; Fig. 1) have lower positive anomalies of these elements,

and lack a positive anomaly at K. Section A falls somewhere between the two; generally, its positive anomaly at K does not exceed values of B, D, and E, though one A section sample shows a negative K anomaly, possibly due to removal of K thorough alteration.

### FRACTIONATION AND CONTAMINATION

Mg-numbers are too low for the rocks to represent primary magmas. Most of the variation in chemistry can be explained by fractional crystallization. Decreasing Ni with decreasing MgO indicates early fractionation of olivine. Decreasing CaO, CaO/Al<sub>2</sub>O<sub>3</sub>, and Sc with decreasing MgO indicates fractionation of clinopyroxene (Fig. 3). Decreasing Cr with decreasing MgO indicates fractionation of either clinopyroxene or, more likely, spinel. K<sub>2</sub>O, Rb, and Ba are conserved, but a small group of lavas (those in the top of the A section) plot beneath the trend (Fig. 3).

The scarcity of plagioclase phenocrysts, the lack of a negative Eu anomaly, and a positive correlation between CaO/Al<sub>2</sub>O<sub>3</sub> and MgO is common in Cenozoic alkaline magmatism in Asia (Barry et al., 2003, Fan and Hooper, 1998), and suggests plagioclase was not an important part of the fractionating assemblage. However, modeling of fractionation based on simple mass balance calculations, least-squares mass balance analysis, and thermodynamic modeling with COMAGMAT (Almeev et al., 2006; Almeev et al., 2007) all show significant plagioclase fractionation (at least 20%).

Samples from the top of the A section have relatively low K, Ba, and Rb at low MgO. These samples may represent a different melting history than the majority of the lavas. Another possibility is assimilation of crustal materials. However, based on Ce/Pb and La/Nb ratios, little crustal contamination is present in the lavas. Also, low values of Rb in these samples cannot be accounted for this way.

### DEPTH OF MELTING

REE modeling of batch and fractional melting suggests that a small amount of garnet (~5%) must be present in the source area to achieve the displayed depletion in HREE (Fig. 4). Based on this data, the source area can be constrained to the garnet stability field. Ionov et al. (1998) find garnet lherzolite to be stable at depths >70 km for the Tariat region in the Hangay, and the most abundant xenolith, spinel peridotite, to be stable from 50-70 km. Thus, the source of melt must be >70 km.

Barry et al. (2003) argue that melting occurred in a metasomatized, amphibole-enriched, garnet-peridotite source at depths >70 km. Peaks at Sr, K, and Ba are consistent with a metasomatized source. Presence of amphibole is not confirmed (no positive Nb anomaly), but not precluded.

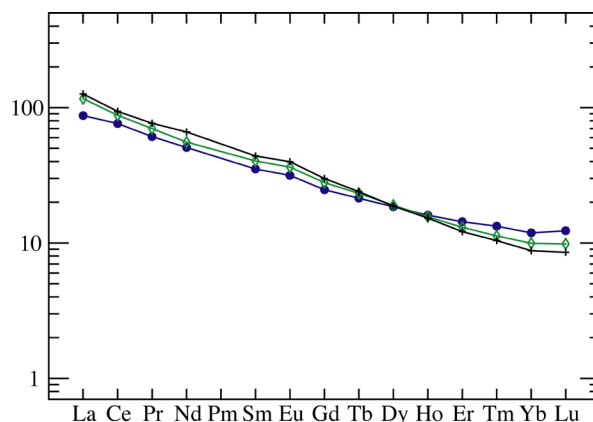


**Figure 5. Representative whole-rock rare earth element concentrations normalized to chondrite (after Sun and McDonough, 1989). Blue filled circles, B flow; green open diamonds, E cone; black crosses, H section.**

### CONCLUSIONS

Overall, little chemical variation occurs in Mongolian lavas, despite differing spatial distributions and age constraints. This is consistent with previous workers' results. Samples from Tielke et al. (this volume) match closely with samples from this study, as do general trends of data from Barry et al. (2003). All lavas come from a garnet-bearing region,

with a depth of melting >70 km. Fractional crystallization explains most of the variation in chemistry. Isotope data is needed to confirm the results found here, and radiometric dating would better constrain the relative ages of the widely separated lavas in this study.

A mantle plume is an unlikely explanation for the generation of these basalts. Plume activity would be expected to generate changes in chemistry over time and location. Such temporal and spatial variation is not seen in this study.

Barry et al. (2003) suggest two models for generation of melting. The first model calls for a thermal anomaly causing melt infiltration leading to metasomatism, with three possible sources of excess thermal energy: a mantle plume for which only the shallow cooling lens remains (unlikely since early volcanism was not more voluminous), a deep plume feeding laterally into thinspots, or thermal blanketing of the Eurasian continent allowing the upper mantle to warm in response to convection. The second model considers Mesozoic magmatic activity as a possible cause of metasomatic enrichment, proposing that such activity may have weakened the lithosphere, leading to lithospheric delamination. Further investigation is needed to determine which of these is more likely.

## REFERENCES

- Almeev, R.R., Holtz, F., Koepke, J., and Parat, F., 2006, The effect of small amount of H<sub>2</sub>O on liquidus of olivine, plagioclase and clinopyroxene: An experimental study at 200 and 500 MPa: *Experimental Mineralogy, Petrology, and Geochemistry*, 11th International Conference, University of Bristol, UK, Abstracts, p. 4.
- Almeev, R.R., Holtz, F., Koepke, J., Parat, F., and Botcharnikov, R., 2007, The effect of H<sub>2</sub>O on olivine crystallization in MORB: Experimental calibration at 200 MPa: *American Mineralogist* (in press).
- Barry, T.L., Saunders, A.D., Kempton, P.D., Windley, B.F., Pringle, M.S., Dorjnamjaa, D., and Saandar, S., 2003, Petrogenesis of Cenozoic basalts from Mongolia: Evidence for the role of asthenospheric versus metasomatized lithospheric mantle sources: *Journal of Petrology*, v. 44, p. 55-91.
- Devyatkin, Y.V., and Smelov, S.B., 1980, Position of basalts in the Cenozoic sedimentary sequence of Mongolia: *International Geology Review*, v. 22, p. 307-317.
- Fan, Q., and Hooper, P.R., 1991, The Cenozoic basaltic rocks of Eastern China: Petrology and chemical composition: *Journal of Petrology*, v. 32, p. 765-810.
- Ionov, D.A., O'Reilly, S.Y., and Griffin, W.L., 1998, A geotherm and lithospheric section for Central Mongolia (Tariat Region): *in* Flower, M.F.J., Chung, S.-L., Lo, C.-H., and Lee, T.-Y., eds., *Mantle dynamics and plate interactions in East Asia*, *Geodynamics Series*, v. 27: Washington, D.C., American Geophysical Union, p. 127-153.
- Le Bas, M.J., Le Maitre, R.W., Streckeisen, A., and Zanettin, B., 1986, A chemical classification of volcanic rocks based on the total alkali-silica diagram: *Journal of Petrology*, v. 27, p. 745-750.
- Sun, S.-s., and McDonough, W.F., 1989, Chemical and isotopic systematics of oceanic basalts: implications for mantle composition and processes: *in* Saunders, A.D., and Norry, M.J., eds., *Magmatism in the ocean basins: Geological Society Special Publication* 42, p. 313-345.